Article

Cell Host & Microbe

Fungal Mimicry of a Mammalian Aminopeptidase Disables Innate Immunity and Promotes Pathogenicity

Graphical Abstract

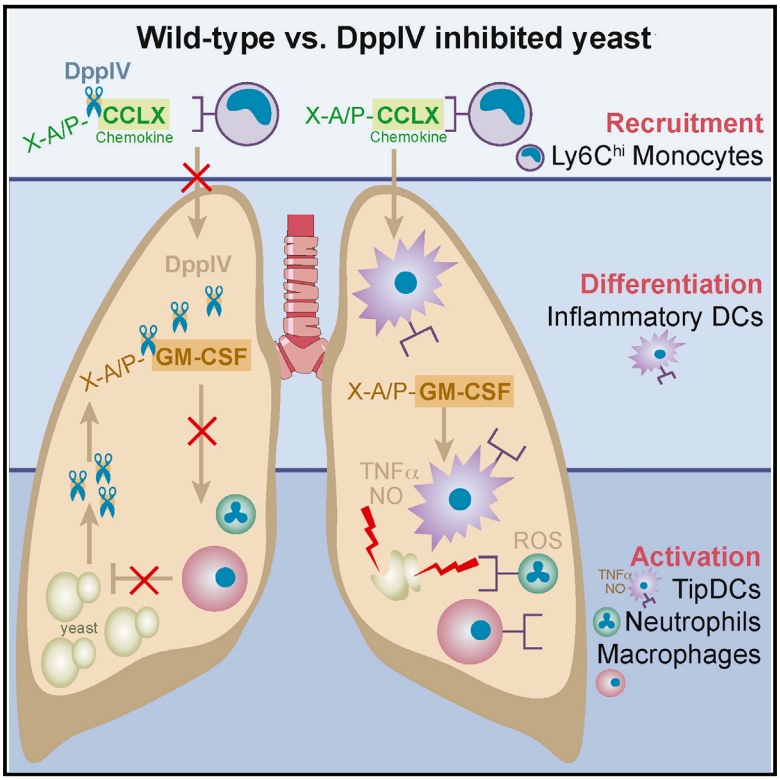

Highlights

- A fungal protease, DppIVA, cleaves and inactivates host cytokines and chemokines
- Fungal DppIVA blunts recruitment, differentiation, and activation of Ly6c^{hi} monocytes
- Fungal protease cleavage of GM-CSF tempers activation of a variety of leukocytes
- An FDA-approved inhibitor of DppIV ameliorates progressive fungal lung infection

Authors

Alana K. Sterkel, Jenna L. Lorenzini, J. Scott Fites, ..., Nydiaris Hernandez-Santos, George S. Deepe, Jr., Bruce S. Klein

Correspondence

bsklein@wisc.edu

In Brief

Mammalian proteases regulate the immune response by altering the activity of cytokines and chemokines. Here, Sterkel, Lorenzini, and colleagues identify a fungal protease that promotes virulence and suppresses innate immunity to infection by mimicking the immune-modulatory activity of its mammalian counterpart.

Sterkel et al., 2016, Cell Host & Microbe *19*, 361–374
March 9, 2016
http://dx.doi.org/10.1016/j.chom.2016.02.001

Cell Host & Microbe
Article

Fungal Mimicry of a Mammalian Aminopeptidase Disables Innate Immunity and Promotes Pathogenicity

Alana K. Sterkel,[1,3] Jenna L. Lorenzini,[1,3] J. Scott Fites,[1] Kavitha Subramanian Vignesh,[2] Thomas D. Sullivan,[1] Marcel Wuthrich,[1] Tristan Brandhorst,[1] Nydiaris Hernandez-Santos,[1] George S. Deepe, Jr.,[2] and Bruce S. Klein[1,*]
[1]Departments of Pediatrics, Medicine, and Medical Microbiology and Immunology, School of Medicine and Public Health, University of Wisconsin-Madison, Madison, WI 53726, USA
[2]Division of Infectious Disease, University of Cincinnati College of Medicine and Veterans Affairs Hospital, Cincinnati, OH 45220, USA
[3]Co-first author
*Correspondence: bsklein@wisc.edu
http://dx.doi.org/10.1016/j.chom.2016.02.001

SUMMARY

Systemic fungal infections trigger marked immune-regulatory disturbances, but the mechanisms are poorly understood. We report that the pathogenic yeast of *Blastomyces dermatitidis* elaborates dipeptidyl-peptidase IVA (DppIVA), a close mimic of the mammalian ectopeptidase CD26, which modulates critical aspects of hematopoiesis. We show that, like the mammalian enzyme, fungal DppIVA cleaved C-C chemokines and GM-CSF. Yeast producing DppIVA crippled the recruitment and differentiation of monocytes and prevented phagocyte activation and ROS production. Silencing fungal *DppIVA* gene expression curtailed virulence and restored recruitment of CCR2^{+} monocytes, generation of TipDC, and phagocyte killing of yeast. Pharmacological blockade of DppIVA restored leukocyte effector functions and stemmed infection, while addition of recombinant DppIVA to gene-silenced yeast enabled them to evade leukocyte defense. Thus, fungal DppIVA mediates immune-regulatory disturbances that underlie invasive fungal disease. These findings reveal a form of molecular piracy by a broadly conserved aminopeptidase during disease pathogenesis.

INTRODUCTION

Pathogenic fungi have been dubbed the hidden killers due to the mounting rates of fungal infections. Immune-compromised patients such as those with AIDS, organ transplants, and cancer and chemotherapy are among those at risk of serious fungal infections. The endemic dimorphic fungi are primary pathogens that collectively account for nearly one million systemic infections annually in North America (Pfaller and Diekema, 2010). These agents infect previously healthy individuals but can also reactivate from a latent state when immunity is impaired. Among these systemic mycoses, the proportion of immune-competent persons with symptomatic illness varies according to pathogen. At one end of the spectrum, about 50% become overtly ill after infection with *Blastomyces dermatitidis* (Klein et al., 1986), whereas about 10% manifest clinically significant illness with *Histoplasma capsulatum* (Ward et al., 1979). The high ratio of illness to infection and the potential severity of disease underscore the pathogenic and immune-evasive potential of dimorphic fungi and make them challenging pathogens from a clinical vantage point.

Several factors have been linked to virulence in dimorphic fungi (Rappleye and Goldman, 2008). Some include calcium binding protein (CBP) and superoxide dismutase (SOD) in *H. capsulatum*, glucan synthase in *Coccidioides* sp., α-1,3-glucan and Drk1 (dimorphism-regulating kinase) in several members, and *Blastomyces* adhesin-1 (BAD-1) in *B. dermatitidis*. Immune dysregulation is a hallmark of infections with dimorphic fungi, but there is limited insight about how fungal factors subvert immunity. SOD protects *Histoplasma* from oxidative stress (Youseff et al., 2012), and surface α-1,3-glucan shields this fungus from recognition by dectin-1 (Rappleye et al., 2007). BAD-1 has multiple functions: it mediates binding of *Blastomyces* to macrophages and lung tissue, modulates expression of host TNF-α and TGF-β, binds calcium and other divalent cations, and impairs T cell activation and function by engaging heparin sulfate modifications of surface CD47 (Brandhorst et al., 2013).

Failure of vaccination at the lung mucosa reveals features of immune dysregulation induced by dimorphic fungi. An attenuated, BAD-1 deletion strain of *B. dermatitidis*, which protects against lethal experimental blastomycosis when given subcutaneously, fails to protect when given via the respiratory route (Wüthrich et al., 2012). Vaccine delivery at the respiratory mucosa induces a host immune regulatory circuit, which hampers the recruitment of Ly6C^{hi} monocytes into the lungs and undermines the priming of antigen-specific CD4^{+} T cells within this compartment.

Ly6C^{hi} monocytes recruited to sites of inflammation play a key role in the control of infections due to bacteria (e.g., *Listeria monocytogenes*), parasites (e.g., *Toxoplasma gondii*), and fungi (e.g., *Cryptococcus neoformans*, *Aspergillus fumigatus*, and *H. capsulatum*) (Serbina et al., 2003, 2008). Upon arrival in tissue, Ly6C^{hi} inflammatory monocytes have the ability to differentiate into macrophage and inflammatory dendritic cells (DCs),

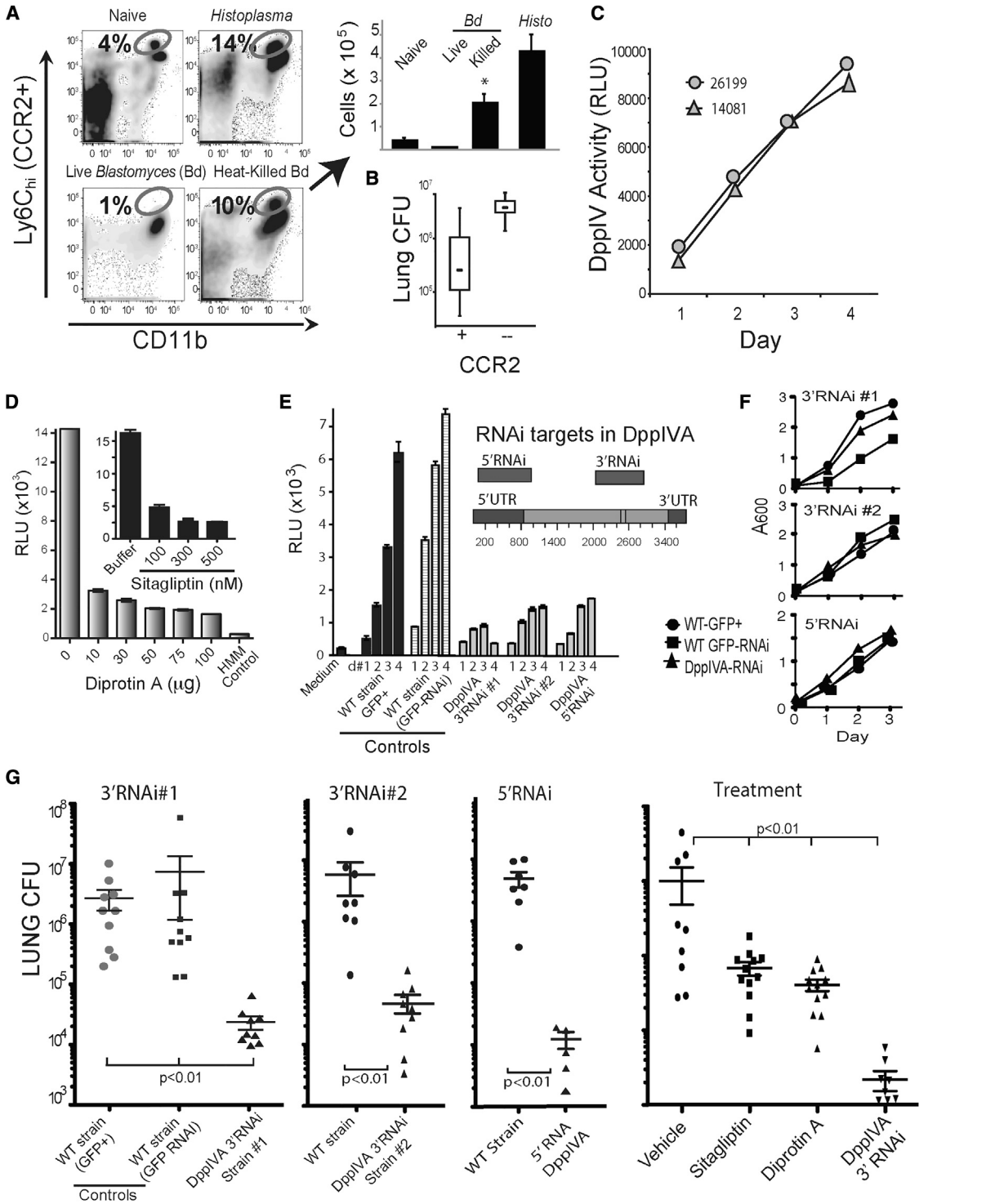

Figure 1. DppIVA Blunts Recruitment of Ly6c^{hi} CCR2$^+$ Monocytes to the Lung and Promotes *B. dermatitidis* Virulence

(A) Ly6c^{hi} CCR2$^+$ monocytes (circled population) recruited to the lungs of mice 4 days after infection with *Histoplasma* yeast, or live versus heat-killed *Blastomyces* yeast.

(B) Lung CFU 7 days postinfection in WT or *Ccr2*$^{-/-}$ mice infected with *Blastomyces* yeast.

(C) Glo assay of DppIV activity in culture supernatant of two strains of *Blastomyces* yeast grown in vitro. RLU, relative fluorescence unit.

(D) Seven-day culture supernatant of yeast tested for DppIV activity in the presence of DppIV inhibitors diprotin A (Ile-Pro-Ile) or sitagliptin. HMM, medium control.

(E) *DppIVA* 3′ and 5′ regions silenced by RNAi (inset) and DppIV activity (RLU × 10^3) in supernate of isogenic strains as follows: WT GFP$^+$ parental, WT-GFP (only)-RNAi, and DppIVA-RNAi yeast.

(legend continued on next page)

including a subset termed TipDC (TNF-α- and iNOS-producing dendritic cells) (Serbina et al., 2003). The potent immune modulatory effects of TNF-α and powerful killing products generated with iNOS make these cells forceful effectors against invading pathogens. Thus, a paucity of Ly6C^{hi} monocytes at sites of inflammation during host: pathogen interactions could undermine immunity in ways beyond the failure to prime antigen-specific T cells.

Ly6C^{hi} monocytes exit the bone marrow in response to soluble C-C chemokine signals received through their G protein-coupled receptor CCR2 (Serbina et al., 2008). The chief signals in mice are CCL2, CCL7, and CCL12. We previously reported that CCL7 was elevated in the serum of mice that received the vaccine strain of *Blastomyces* at the respiratory mucosa (Wüthrich et al., 2012). However, naive CCR2^{+}Ly6C^{hi} monocytes failed to migrate in response to these sera in vitro, implying that the C-C chemokine was not functional. Likewise, Ly6C^{hi} cells from vaccinated mice migrated poorly in response to recombinant CCL7, implying desensitization of CCR2, which was supported by reduced calcium flux in response to ligand-induced triggering of CCR2 in the cells. We found evidence that vaccine induction of lung matrix metalloproteinase-2 (MMP2) and its action on CCL7 accounted for blunted recruitment of Ly6C^{hi} cells and failed priming of CD4 T cells.

MMP2 is capable of cleaving five residues from the N terminus of CCL7, which inactivates the chemokine, converts it to an antagonist on CCR2, and desensitizes the receptor (Ali et al., 2005). We found that chemical inhibition of MMP2, vaccination of *MMP2*$^{-/-}$ mice, and delivery of CCL7 to mice helped vaccine priming of T cells in the lungs (Wüthrich et al., 2012). However, we could not induce levels of CD4^{+} T cell priming achievable by yeasts that strongly recruit Ly6C^{hi} cells into the lungs, e.g., *H. capsulatum*. Our findings implied that *Blastomyces* products, in addition to host MMP2, may also blunt recruitment of Ly6C^{hi} cells to the lungs. If so, such factors could impact the host: fungal pathogen interaction and contribute to immune dysregulation and progressive infection.

Microbes produce extracellular proteases that mediate virulence (Ingmer and Brøndsted, 2009). Here, we investigated whether a *Blastomyces* serine protease blunts influx or function of leukocytes at sites of inflammation and impacts pathogenesis of disease. We asked three questions: (1) is yeast viability needed to modulate leukocyte recruitment, and, if so, what products mediate the action; (2) what role is played by the serine protease di-peptidyl peptidase IVA (DppIVA) in modulating leukocyte influx into the lungs, inflammation, and virulence of *B. dermatitidis*; and (3) how might DppIVA exert its action in blunting the recruitment and function of leukocytes?

We report that *B. dermatitidis* releases extracellular DppIVA, which curtails the influx of Ly6C^{hi} cells into the lungs and impairs the downstream effector functions of these and other leukocytes required for innate defense. We show that DppIVA targets and cleaves C-C chemokines and GM-CSF (granulocyte-macrophage colony-stimulating factor), which has deleterious consequences for the control of infection. Our work establishes a prominent and unappreciated role for microbial DppIVA in pathogen virulence, involving modes of action that mimic the mammalian enzyme CD26, an ectopeptidase known to modulate critical aspects of hematopoiesis. Aminopeptidases are widely conserved among pathogenic microbes, including bacteria, parasites, and fungi, and may represent a strategy by which pathogens undermine mammalian innate host defenses.

RESULTS

A Yeast Factor Blunts Leukocyte Recruitment

We explored the role of fungal factors in failed recruitment during primary infection. Live, WT (wild-type) yeast blunted the recruitment of Ly6C^{hi} CCR2^{+} monocytes, but heat killing the yeast led to an increase in Ly6C^{hi} CCR2^{+} monocyte recruitment (Figure 1A), suggesting that a heat-labile factor from the fungus contributes to blunted recruitment of Ly6C^{hi} CCR2^{+} monocytes. We assessed whether CCR2^{+} cells are required to control infection and found that the fungal burden is one to two logs higher in *Ccr2*$^{-/-}$ mice versus WT mice by 7 days after infection (Figure 1B). Thus, blunting the recruitment of CCR2^{+} cells enhances the virulence of WT *B. dermatitidis*.

Mammalian DppIV can cleave and inactivate chemokines and other cytokines responsible for the recruitment and activation of multiple leukocyte populations due to the presence of target proline or alanine residues at the penultimate position of these signals (Boonacker and Van Noorden, 2003). We identified two *DppIV* homologs in the *B. dermatitidis* genome, *DppIVA* and *DppIVB*. The former harbors a secretion signal and is likely secreted, while the latter has a predicted transmembrane domain and is presumed to be intracellular. We tested yeast supernatant for DppIV enzymatic activity and detected activity that increased during growth in vitro (Figure 1C). Selective DppIV inhibitors diprotin A and sitagliptin blocked the generation of signal, indicating that the supernatant activity is due to DppIV (Figure 1D). Mice also express DppIV (CD26), but *B. dermatitidis* yeast suppress phagocyte CD26 expression, while mice exposed to WT yeast mount an antibody response to fungal DppIV in vivo (Figures S1A and S1B, available online), suggesting that the fungal product also is expressed during infection.

DppIVA and Fungal Virulence

We silenced expression of *DppIVA* and *DppIVB* in *B. dermatitidis* yeast. We generated silenced strains using a GFP-RNAi sentinel system for gene silencing (Krajaejun et al., 2007). Briefly, a GFP^{+} strain is transformed with a plasmid harboring inverted hairpins for RNAi silencing of both the gene target and the sentinel GFP. The resulting DppIVA RNAi strain showed reduced expression of GFP and the gene of interest; the DppIVB RNAi strain was unstable, and GFP silencing could not be maintained. We silenced *DppIVA* by targeting the 3′ region and 5′ region and confirmed that DppIVA-silenced strains had reduced DppIV

(F) Growth rate of isogenic DppIVA-silenced and control strains.

(G) Lung CFU of mice infected with WT GFP^{+} parental and RNAi silenced yeast 2 weeks postinfection. Right panel shows lung CFU 7 days postinfection in mice that received WT yeast plus indicated treatment. Six to ten mice/group. Results are representative of three experiments. See also Figure S6.

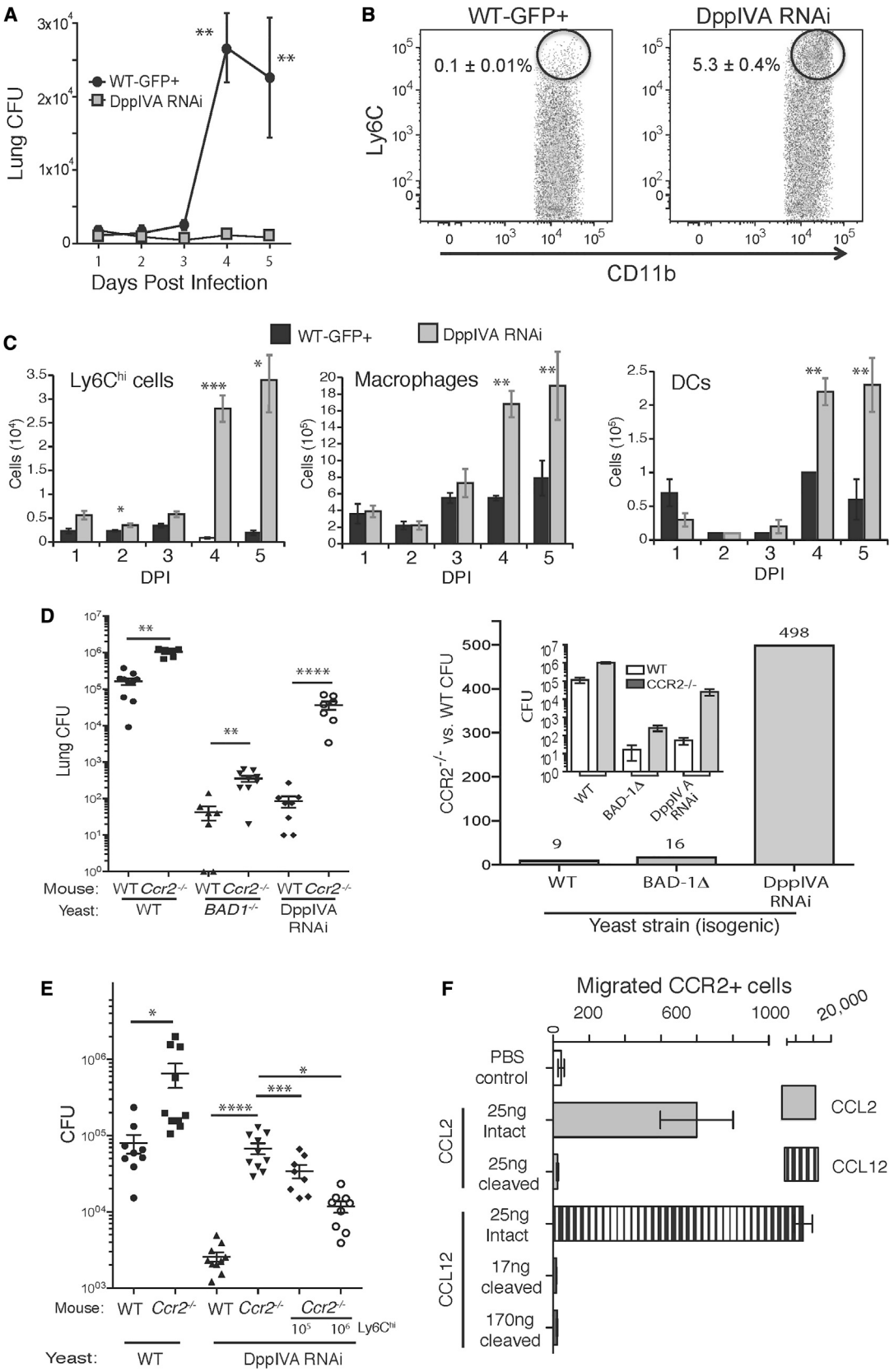

(legend on next page)

enzymatic activity (Figure 1E). The growth rate in vitro of DppIVA RNAi strains was comparable to isogenic WT GFP$^+$ strains and GFP-RNAi strains (Figure 1F). In a murine model of infection, lung CFU (colony-forming unit) was reduced by two to three logs with DppIVA RNAi yeast versus WT controls (Figure 1G). Similar results were observed for multiple independent DppIVA tranformants silenced at the 3′ region or 5′ region. No perturbations in expression of *DppIVB* transcript were detected by RT-PCR in DppIVA RNAi strains (data not shown). Thus, silencing *DppIVA* at multiple regions within the gene, and in multiple independent transformants, attenuated pathogenicity. Likewise, pharmacologic inhibition of DppIV with sitagliptin or diprotin A ameliorated infection in mice that received WT yeast (Figure 1G). DppIVA thus appears essential for virulence in *B. dermatitidis*.

DppIVA and Blunted Ly6C^{hi} Cell Recruitment

We tested a link between *B. dermatitidis* DppIVA and blunted Ly6C^{hi} cell recruitment during infection. We analyzed CFU and the influx of leukocytes to the lung over 5 days postinfection (Figures 2A–2C). Ly6C^{hi} cell recruitment to the lungs was greater in mice infected with DppIVA RNAi yeast than WT yeast. These recruitment differences were evident by the second day of infection (Figure 2C). The numbers of inflammatory macrophages and DCs were also increased in mice infected with the DppIVA RNAi strain, even though the lung CFU was significantly lower in these mice (Figure 2C).

Ly6C^{hi} monocytes are recruited to sites of infection via CCR2 (Serbina et al., 2008). To test whether DppIVA is functionally linked with Ly6C^{hi} monocyte recruitment, we analyzed the progression of infection of DppIVA-silenced yeast in *Ccr2*$^{-/-}$ mice. If linked, the attenuation of DppIVA-RNAi yeast should be "suppressed" and lung CFU greatly increased in *Ccr2*$^{-/-}$ mice. The infection with DppIVA RNAi yeast progressed significantly more in *Ccr2*$^{-/-}$ versus WT mice (Figure 2D), resulting in a 498-fold increase in CFU. This increase in fungal burden with DppIVA RNAi yeast was much greater than with WT yeast or with another (isogenic) attenuated strain of *B. dermatitidis (BAD1*$^{-/-}$) (9- to 16-fold increases), indicating a link between DppIVA and virulence in *Ccr2*$^{-/-}$ mice rather than a general impairment of resistance in the mice.

Although Ly6C^{hi} monocyte recruitment to the lungs was blunted during infection in *Ccr2*$^{-/-}$ mice, adoptive transfer of Ly6C^{hi} cells into *Ccr2*$^{-/-}$ mice significantly reduced the burden of lung infection with DppIVA RNAi yeast (Figure 2E). Thus, Ly6C^{hi} cells restrain infection with DppIVA RNAi yeast, which supports a "gene-to-gene" link between *DppIVA* in the fungus and *CCR2* in the host, leading to blunted recruitment of Ly6C^{hi} cells.

Ly6C^{hi} monocytes are recruited to the lungs via CCR2 and its ligands, CCL2, CCL7, and CCL12. We measured these chemokines in the lung, BAL (bronchoalveolar lavage), and serum and found that they were similar in mice infected with WT versus DppIVA RNAi yeast (Figure S1D; data not shown). Thus, differing chemokine levels do not account for blunted cell recruitment, suggesting functional differences in chemokine action between the two groups. We tested this concept by assaying CCR2$^+$ cell migration in response to intact versus fungal DppIVA-cleaved C-C chemokines. Trimming two amino acids from N terminus of these C-C chemokines, as confirmed by mass spectrometry (MS), impaired the ability of CCR2 to induce migration of reporter cells (Figure 2F) and of primary Ly6C^{hi} cells (Figure S1C). Lung MMP2 levels were >3-fold higher in mice that received WT yeast versus DppIVA RNAi yeast (data not shown), and pharmacological inhibition of MMP2 further augmented influx of Ly6C^{hi} cells in these mice (Figure S1C). Thus, our Ly6C^{hi} results can best be explained by cleavage and inactivation of one or more chemokines by DppIVA, together with elevated MMP2 and desensitized CCR2, as described (Wüthrich et al., 2012).

Enzymatic Action of Fungal DppIVA on GM-CSF and Downstream Effects

GM-CSF promotes differentiation of Ly6C^{hi} cells into DCs in vivo and in vitro (Hamilton, 2008). We found that inflammatory (Ly6C^{hi}) DCs and TipDCs accumulated in greater numbers in the lungs of mice infected with DppIVA RNAi yeast versus WT yeast (Figures 3A and 3B). GM-CSF expression was similarly upregulated during infection with both strains of *B. dermatitidis* (Figure 3C). However, GM-CSF harbors a penultimate proline at the N terminus and is cleaved and inactivated by mammalian DppIV (Broxmeyer et al., 2012). We tested whether *B. dermatitidis* DppIVA cleaves GM-CSF in vitro. By 6 hr of incubation, DppIVA had fully removed both N-terminal residues from GM-CSF in the presence or absence of serum (Figure 3D), and digestion was blocked by the DppIV inhibitor diprotin A. WT yeast cultured in serum (without mammalian cells and CD26) also cleaved GM-CSF (Figure 3E). Since cleaved GM-CSF has diminished action on its receptor (Broxmeyer et al., 2012), the loss of GM-CSF action could have untoward effects in vivo due to impaired differentiation of DC or activation of other leukocytes.

We tested the link between fungal DppIVA and GM-CSF in vivo during infection. We hypothesized that DppIVA cleavage of GM-CSF in vivo would promote immune evasion by WT yeast and, conversely, that loss of DppIVA would enhance GM-CSF-mediated clearance of a DppIVA RNAi strain. If true, growth of the latter strain would be preferentially enhanced in mice lacking

Figure 2. The Inflammatory Response to Yeast that Express DppIVA and the Role of CCR2$^+$ Monocytes

(A) Lung CFU of mice infected with isogenic DppIVA-sufficient and DppIVA-deficient yeast over 5 days.

(B and C) (B) Percentage of Ly6C^{hi} CCR2$^+$ cells in the lungs 3 days postinfection (events shown are those from the CD11b$^+$ Ly6G$^-$ gate) and (C) total number of Ly6C^{hi} cells in lungs. Also shown are the numbers of lung exudative macrophages and DCs. Data are mean ± SEM of five mice/group and representative of three experiments.

(D) WT and *Ccr2*$^{-/-}$ mice were infected with isogenic yeast and analyzed for lung CFU 2 weeks postinfection (left). The mean CFU data (inset) are expressed as fold change between *Ccr2*$^{-/-}$ and WT mice (right).

(E) Ly6C^{hi} cells recruited to lungs and regional lymph nodes of WT mice (infected with DppIVA RNAi yeast) were transferred into *Ccr2*$^{-/-}$ mice infected with DppIVA-silenced yeast. Lung CFU is shown 7 days postinfection. Data are mean ± SEM of eight to ten mice/group. Results are representative of two experiments.

(F) Transwell migration of CCR2$^+$ cells in response to intact or fungal DppIVA-cleaved C-C chemokines. Migration was quantified after 16–24 hr of incubation. Results are representative of two experiments. *$p < 0.05$, **$p < 0.01$, ***$p < 0.001$, ****$p < 0.0001$. See also Figure S1.

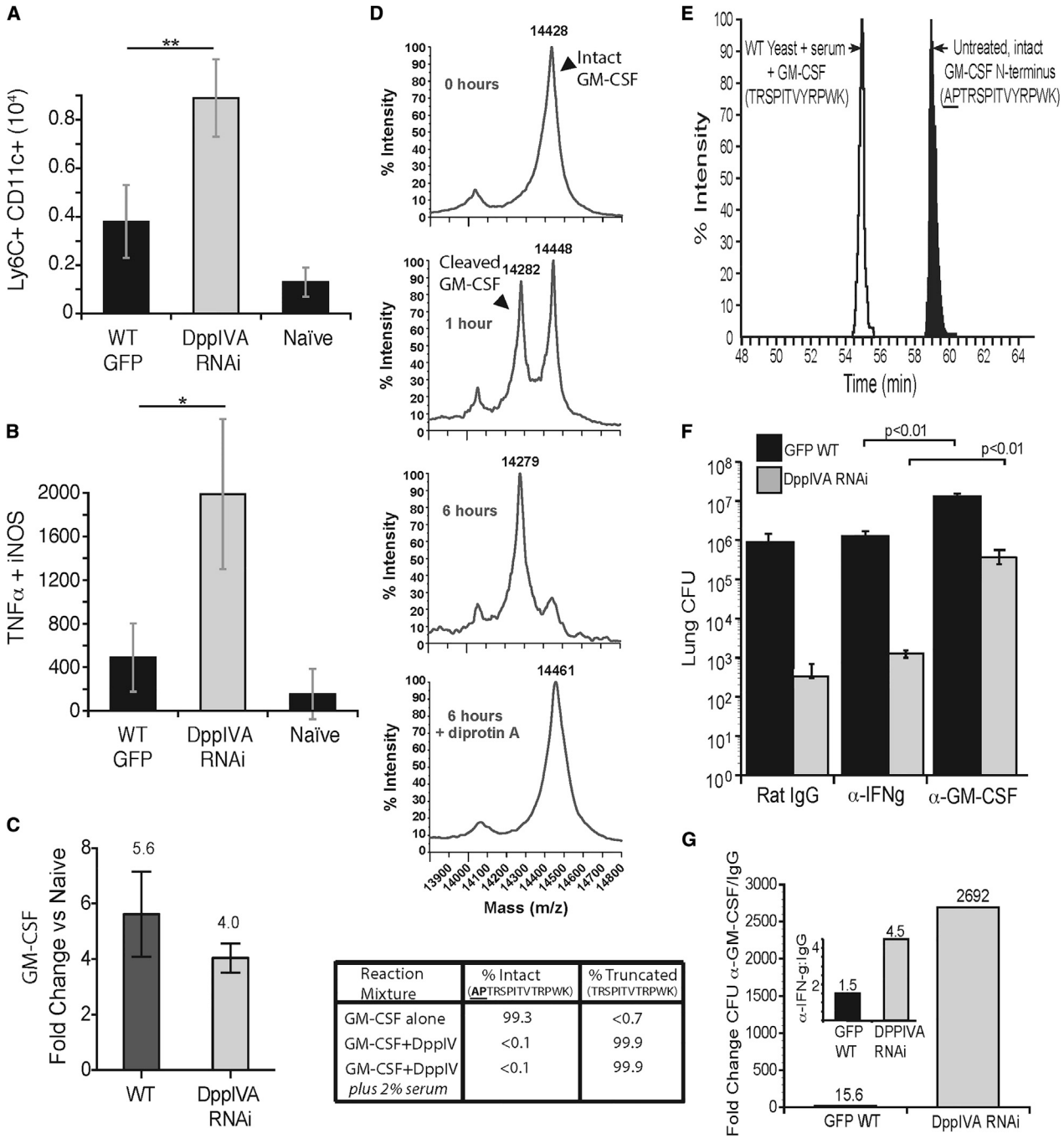

Reaction Mixture	% Intact (APTRSPITVTRPWK)	% Truncated (TRSPITVTRPWK)
GM-CSF alone	99.3	<0.7
GM-CSF+DppIV	<0.1	99.9
GM-CSF+DppIV *plus 2% serum*	<0.1	99.9

Figure 3. Action of Yeast DppIVA on GM-CSF and Impact on Evolution of Infection

(A and B) Number of monocyte-derived DCs ($CD11c^+$, $Ly6C^{hi}$ cells) (A) and TipDCs (TNF-α, $NOS2^+$, $CD11c^+$, $Ly6C^{hi}$) (B) in the lungs 4 days postinfection. *$p < 0.05$, **$p < 0.01$.

(C) Fold increase in transcript of GM-CSF measured by RT-PCR in lung homogenate 2 days postinfection compared to naive mice. Data in (A)–(C) are mean ± SEM of three to five mice/group and are representative of two experiments.

(D) MS analysis of GM-CSF cleavage by fungal rDppIVA at 0, 1, and 6 hr of incubation alone or with diprotin A. Table shows extent of removal of N-terminal two amino acids (AP) by rDppIVA in buffer alone or with 2% serum.

(E) WT yeasts were cultured in vitro in medium with GM-CSF and 2% mouse serum. After 72 hr, GM-CSF was collected by chromatography and analyzed by MS for residues at the N terminus (open peak) versus untreated GM-CSF (shaded peak).

(F) Mice received rat IgG or neutralizing α-GM-CSF or α-IFN-γ and were infected with yeast strains, and lung CFU was enumerated as above in (E).

(G) Fold change in CFU between GM-CSF-neutralized versus rat IgG-treated mice is shown for each yeast strain. Inset shows fold change for rat IgG-treated versus IFN-γ-neutralized mice. Numbers above bars are fold change.

Data in (E) and (F) are mean ± SEM of 8–10 mice/group and are representative of two experiments. See also Figure S4.

this cytokine. To test this hypothesis, we neutralized GM-CSF during infection (Figures 3F and 3G). Lung CFU in mice infected with the DppIVA RNAi strain was sharply elevated compared to infection with WT yeast in GM-CSF-neutralized mice. In contrast, neutralization of IFN-γ (not expected to be a substrate of DppIVA) had a negligible effect on infection by both yeast strains (Figure 3G). In a second approach, we infected GM-CSF-receptor knockout (*Csf2ra*$^{-/-}$) mice with WT or DppIVA RNAi yeast. The absence of GM-CSF receptor signaling in *Csf2ra*$^{-/-}$ mice significantly increased growth of the DppIVA RNAi strain by 12,098-fold, while growth of the WT strain was increased by 1,166-fold (Figure S4A). The increased growth of the WT strain in *Csf2ra*$^{-/-}$ mice suggests incomplete cleavage of GM-CSF by fungal DppIVA in WT mice. Thus, DppIVA is functionally linked with GM-CSF in vivo, implying that inactivation of the cytokine during infection with WT yeast is essential for pathogen virulence.

Analysis of Host: Pathogen Encounters In Vivo with a Reporter Strain of Yeast

We engineered a DsRed reporter strain of *B. dermatitidis* to track yeast encounters with host leukocytes in vivo and assess their impact on yeast survival, i.e., which cells associate with and kill yeast. DsRed signal is strong in viable yeast and absent in dead yeast (Figure 4A). The DsRed signal correlates with CFU (Figures 4A and S2A), as reported for *A. fumigatus* (Jhingran et al., 2012). During coculture in vitro with DsRed yeast, TipDCs killed better than monocytes or macrophages and required iNOS for killing (Figures 4B and S2B). By using uvitex to stain cell-wall chitin and detect all yeast in vivo, e.g., live and dead (Figure 4C), we defined the identity of leukocytes associated with yeast and the ability of different leukocytes to kill them during infection. Dead yeast were more often associated with TipDCs than with Ly6C^{hi} monocytes or Ly6C^{+} cell-derived macrophages in vivo (Figure 4D). To test the role of TipDCs as a cellular basis for the loss of immune control of the silenced yeast, we transferred Ly6C^{hi}-derived inflammatory DCs into *Ccr2*$^{-/-}$ mice infected with DppIVA RNAi yeast. Addition of these DCs (capable of producing iNOS and TNF-α when stimulated with yeast; Figure S2B; data not shown) enhanced the killing of DsRed yeast in vivo and did so in a manner dependent on iNOS, but not TNF-α (Figure 4E). Thus, TipDCs are potent effectors in vivo, and yeast DppIVA undermines their development during infection. However, proportionately more killing of yeast is mediated by macrophages and neutrophils in vivo due to their greater absolute numbers in infected lungs, and these populations also are more active against DppIVA RNAi yeast versus WT yeast in vivo (Figure 4F). We studied each of these leukocyte populations further below.

DppIVA Promotes Survival of Yeast in GM-CSF-Activated Macrophages

To further assess how DppIVA production by yeast provides a survival advantage to the pathogen, we cocultured bone-marrow-derived macrophages with WT or DppIVA RNAi yeast in the presence of GM-CSF. GM-CSF induced meager growth inhibition of WT yeast, but the growth of DppIVA RNAi yeast was inhibited by nearly 60% (Figure 5A). Moreover, blocking DppIV activity with diprotin A boosted growth inhibition of WT yeast to levels near those observed for DppIVA RNAi yeast (Figure 5B). To test whether addition of DppIVA would rescue growth of DppIVA-deficient RNAi yeast, we supplemented culture media with recombinant (r) *Blastomyces* DppIVA. Addition of rDppIVA reversed the growth inhibitory capacity of GM-CSF-activated macrophages and improved the survival of DppIVA RNAi yeast (Figure 5B). GM-CSF-activated macrophages from human donors yielded similar results (Figure S3A). Thus, DppIVA produced by yeast counteracts the antifungal effect of GM-CSF-activated macrophages.

Our in vitro studies revealed that yeast DppIVA impedes the antifungal action of macrophages in the presence of GM-CSF. To validate that GM-CSF regulates the response of macrophages to infection in vivo, we adoptively transferred peritoneal macrophages from WT or *Csf2ra*$^{-/-}$ mice into *Csf2ra*$^{-/-}$ mice just prior to infection with the DppIVA RNAi strain. The transfer of WT macrophages into *Csf2ra*$^{-/-}$ mice sharply enhanced antifungal immunity and decreased growth of the DppIVA RNAi strain in *Csf2ra*$^{-/-}$ mice (Figure 5C). In contrast, transfer of *Csf2ra*$^{-/-}$ macrophages failed to curtail growth of this fungal strain. Adoptive transfer of WT macrophages to *Csf2ra*$^{-/-}$ mice helped control infection with WT yeast as well, but not to the same extent as with DppIVA RNAi yeast (Figure S4B). *Csf2ra*$^{-/-}$ mice possess increased amounts of pulmonary GM-CSF due to lack of signaling via the GM-CSF receptor (Carey and Trapnell, 2010). Introduction of WT macrophages in these mice presumably restored GM-CSF signaling in the transferred cells. Thus, GM-CSF activation of macrophages helps control a dimorphic fungus in vivo, and GM-CSF cleavage and inactivation by DppIVA from WT yeast appears to promote fungal escape from macrophage-mediated killing and progression of disease.

Impact of DppIVA Inactivation of GM-CSF on Neutrophils

GM-CSF is a polyfunctional cytokine; it activates neutrophils and augments their antifungal action (Hamilton, 2008). We hypothesized that fungal DppIVA cleavage of GM-CSF would curtail neutrophil activation and killing of yeast. We found that the number of neutrophils recruited to the lungs during infection was higher in response to WT versus DppIVA RNAi yeast (Figure 6A) and correlated with higher lung CFU by day 4 of infection, although the ratio of neutrophils to yeast was lower in WT infection (Figure S5B). Likewise, a much smaller proportion of the cells displayed an activated phenotype in mice infected with WT versus DppIVA RNAi yeast, as measured by surface expression of CD11b or CD11a and Ly6G (Figures 6B and S5A). Similarly, the two groups of mice showed corresponding differences in neutrophil ROS (reactive oxygen species) production, with less ROS production in the neutrophils from mice infected with WT yeast.

We tested the roles of GM-CSF and fungal DppIVA in neutrophil-mediated killing of yeast in vitro. Addition of GM-CSF to neutrophils in vitro enhanced their killing of DppIVA silenced yeast but did not affect the killing of WT yeast (Figure 6C); killing required GM-CSF receptor on the neutrophils (Figure S4C). Addition of fungal rDppIVA prevented the killing of DppIVA-silenced yeast by GM-CSF-treated neutrophils, lowering the level of killing (10%) to that observed for nontreated neutrophils against WT yeast (Figure 6C). Conversely, addition of the DppIV inhibitor, diprotin A, increased the ability of GM-CSF-treated neutrophils to kill WT yeast (Figure 6C). Diprotin A enhanced

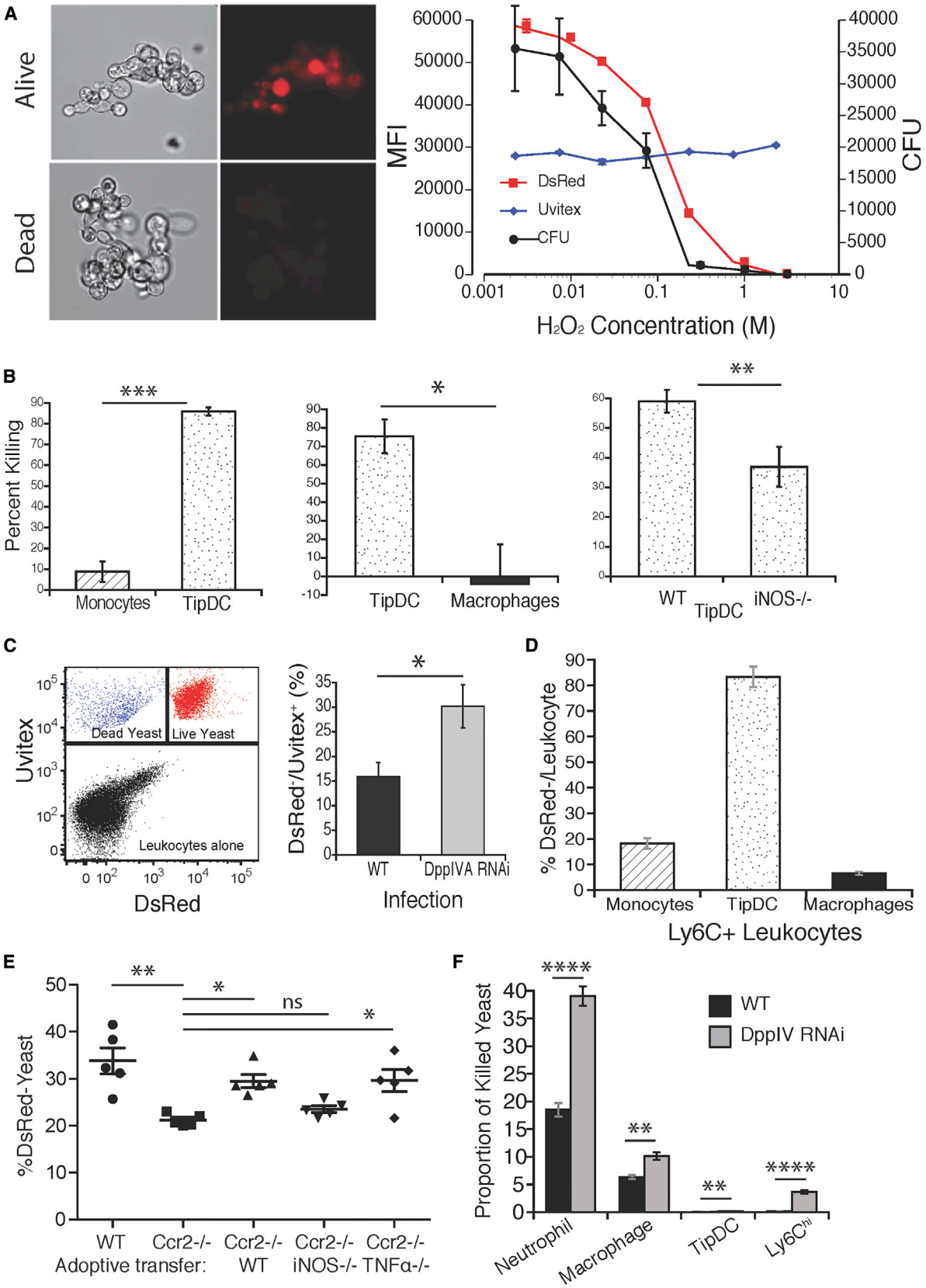

(legend on next page)

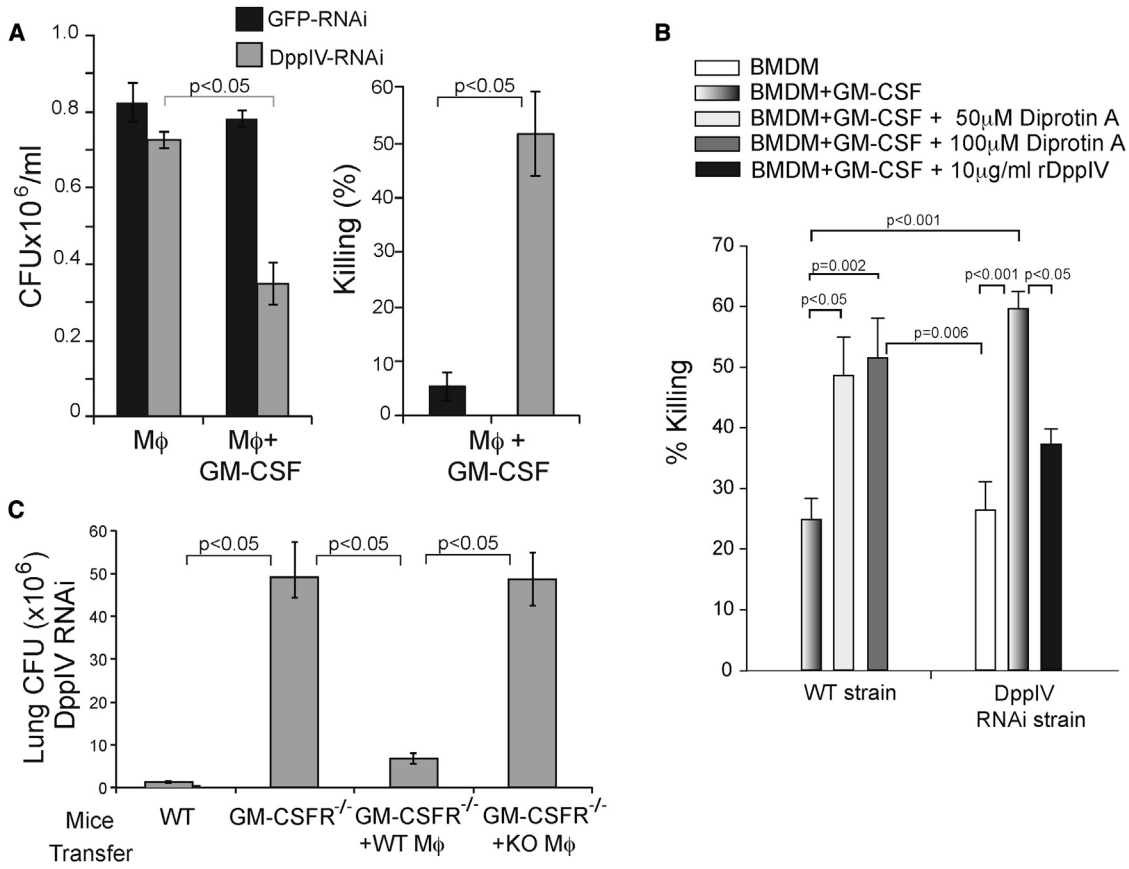

Figure 5. GM-CSF Enhances Killing of Yeast by Macrophages that Is Reversed by Fungal DppIVA

(A) Yeast CFU (left) and percent killing (right) of yeast cultured for 24 hr with GM-CSF-activated, bone-marrow-derived macrophages (BMDM).

(B) Growth inhibition of yeast cultured with GM-CSF-activated BMDM treated with DppIVA or diprotin A.

(C) Lung CFU in *Csf2ra*$^{-/-}$ mice 7 days after infection with DppIVA RNAi yeast and adoptive transfer of WT versus *Csf2ra*$^{-/-}$ peritoneal macrophages. See also Figure S3.

killing of WT yeast in a concentration-dependent manner, yielding levels of killing (25%–30%) similar to that observed by GM-CSF-treated neutrophils against the DppIVA-silenced strain. Neutrophils from human donors mirrored results with murine cells (Figure S3B). Of note, rDppIVA did not directly affect or reduce neutrophil killing of the silenced strain; it did so only in the presence of GM-CSF (Figure S5B). The addition of diprotin A reversed the ability of rDppIVA to suppress killing of silenced yeast by GM-CSF-treated neutrophils (Figure S5B). Neither soluble DppIVA nor diprotin A affected in vitro growth of yeast in the absence of phagocytes (Figure S5C). Thus, fungal DppIVA blunts priming of neutrophils by inactivating GM-CSF, promoting survival of yeast and disease progression.

In murine Aspergillosis, CCR2^{+} monocytes augment neutrophil killing of conidia (Espinosa et al., 2014). We found that the blunted activation state of neutrophils in *Ccr2*$^{-/-}$ mice lacking CCR2^{+} monocytes mirrored that of WT mice infected with WT yeast, in which monocyte recruitment is blunted (Figure 6D). Likewise, although the killing of yeast in vivo in *Ccr2*$^{-/-}$ mice is higher in activated neutrophils than in nonactivated neutrophils,

Figure 4. A Yeast Reporter to Decipher the Host: Fungal Pathogen Encounter In Vivo

(A) *B. dermatitidis* DsRed reporter shows loss of fluorescence in nonviable yeast (left). Loss of DsRed (mean fluorescence intensity, MFI) over increasing [H_2O_2] correlates with CFU, while uvitex signal (cell-wall chitin) persists (right).

(B) DsRed yeasts (DppIVA RNAi strain) were cultured in vitro with cells shown at effector to target ratio of 3:1 for 24 hr, and CFU was recorded to assess percent yeast killed. See similar results for DsRed WT in Figure S2B.

(C) Fluorescent appearance of Uvitex^{+}, dead (DsRed^{-}) versus live (DsRed^{+}) yeast in vivo (left), and the proportions of dead yeast 4 days postinfection with WT and DppIVA RNAi yeast (right).

(D) Percentage of nonviable yeast associated with Ly6C^{hi} monocyte-derived leukocytes 4 days after infection with DppIVA RNAi yeast.

(E) Adoptive transfer of in vitro-elicited WT, *iNOS*$^{-/-}$, and *TNF-α*$^{-/-}$ inflammatory DCs (10^6/recipient) into *Ccr2*$^{-/-}$ mice infected with DsRed, DppIVA-silenced yeast.

(F) Proportion of dead DsRed yeast associated with leukocytes relative to yeast expression of DppIVA. *p < 0.05, **p < 0.01, ***p < 0.001, ****p < 0.0001. See also Figure S2.

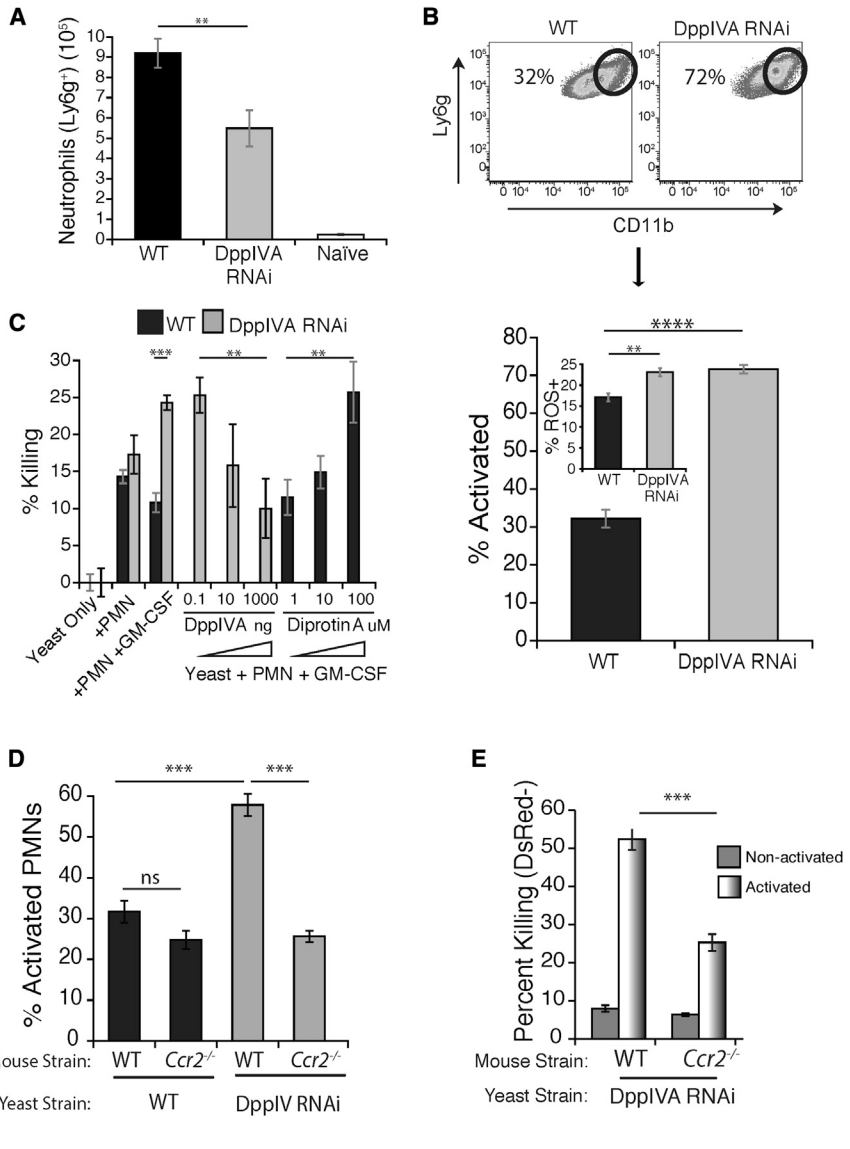

Figure 6. Neutrophil Action against Yeast Is Blunted by Fungal DppIV and Requires Both GM-CSF and Monocyte Recruitment

(A) Number of neutrophils recruited to the lung at day 4 postinfection. Data are mean ± SEM of three to five mice/group and representative of two experiments.

(B) Percentage of neutrophils that are activated ($Ly6G^+$ and $CD11b^{hi}$) in infected mice. Dot plot of lung neutrophils is from a representative mouse (top), and histogram (bottom) is from ten mice/group at 4 days postinfection. Inset shows the percentage of ROS^+ lung neutrophils without ex vivo stimulation in these mice.

(C) Percentage of yeast killed after culture for 6 hr with neutrophils activated with GM-CSF. Some wells contained fungal rDppIVA or DppIV inhibitor diprotin A.

(D and E) (D) Percentage of lung neutrophils activated ($CD11b^{hi}$) at 4 days after infection, illustrating how impaired $CCR2^+$ monocyte recruitment blunts activation of neutrophils and killing (E) of yeast. Data are the mean ± SEM three to five mice/group and representative of two experiments. $^{**}p < 0.01$, $^{***}p < 0.001$, $^{****}p < 0.0001$. See also Figures S5 and S6.

killing by the former is nevertheless sharply impaired in the absence of recruited $CCR2^+$ monocytes (Figure 6E). Adoptive transfer of $Ly6C^{hi}$ monocytes into *Ccr2*$^{-/-}$ mice significantly enhanced the killing of DppIVA RNAi yeast in vivo by neutrophils and neutrophil-DC hybrids, as well as by macrophages (Figure S6). Thus, $Ly6C^{hi}$ monocytes not only can kill the fungal pathogen directly (Figures 4B and 4C) and can differentiate into macrophages and DCs that are even more potent killers, but $Ly6C^{hi}$ monocytes also appear to provide signals to neutrophils and other phagocytes that augment their ability to kill the fungal pathogen.

DISCUSSION

The dimorphic fungi exert profound immune regulatory disturbances during the course of progressive, systemic infection, but little is known about the molecular basis of these defects. We report that fungal DppIVA subverts elements of host innate immunity in a murine model of pulmonary infection with *B. dermatitidis* and accounts for progressive, lethal infection. Conversely, elimination of expression of DppIVA in the pathogen attenuates its virulence and is associated with restoration of early leukocyte recruitment, function, and control of disease. Thus, DppIVA is strongly implicated in these events.

Gene silencing may have off-target effects, limiting the strength of our conclusions. To guard against confounding effects, we took several measures. First, we silenced multiple regions of *DppIVA*, including at the 3′ and 5′ ends. Second, we avoided targeting regions of homology with *DppIVB*. Third, we ensured that *DppIVB* transcript was unaffected in DppIVA-silenced strains and that enzyme activity was specifically reduced in DppIVA-silenced strains. Fourth, to control for random integration of silencing constructs, we studied multiple independent transformants of DppIVA-silenced strains. Fifth, we controlled for the effects of RNAi-silencing machinery by including strains in which only GFP was silenced (i.e., transformants where the transforming DNA had only GFP in the RNAi cassette) and showed that these strains have WT levels of DppIV activity and virulence. Nevertheless, we were unable to obtain a clean, targeted deletion of the *DppIVA* gene in *B. dermatitidis*, offering unambiguous proof. Still, the immune disturbances identified in our study are highly reminiscent of the actions ascribed to mammalian DppIV.

DppIV is a multifunctional protein conserved in mammals and microbes. DppIV is a member of the prolyl oligopeptidase family known for its function as a serine protease, selectively cleaving the N-terminal penultimate proline or alanine from proteins.

The best-studied DppIV is human CD26, which removes dipeptides from chemokines, binds extracellular matrix constituents such as collagen and fibronectin, and interacts with other proteins, such as adenine deaminase on T cells and a Na^+/H^+ antiporter pump on kidney cells (Boonacker and Van Noorden, 2003). Human DppIV cleaves CXCL10 (IP-10) and CXCL12, inactivating these attractants of T cells and hematopoietic stem cells, respectively (Ou et al., 2013). Over 40 cytokines and chemokines display a penultimate proline or alanine and are potentially cleavable by DppIV (Ou et al., 2013). Cleavage of such targets by microbial DppIV could foster immune evasion, but to our knowledge, there are no firm examples of this microbial evasion strategy.

We found that recruitment of $Ly6C^{hi}$ $CCR2^+$ monocytes into the lungs was blunted during infection with WT yeast, but not DppIVA-silenced yeast. The C-C chemokine signals that attract these cells to sites of inflammation include CCL2, CCL7, and CCL12. The lung and serum levels of transcript and protein for these products did not differ in mice infected with these strains, implying a difference in their functional activity in the two settings. Each of these targets displays a penultimate proline target of DppIV cleavage. Removal of several N-terminal residues impairs the activity of these chemokines on CCR2, converts them into antagonists, and desensitizes CCR2 itself.

Pathogenic yeasts may prevent monocyte recruitment through mechanisms other than DppIVA cleavage of CCR2 ligands. DppIVA may indirectly upregulate MMP-2, which can block $Ly6C^{hi}$ monocyte recruitment by cleaving CCL7 (Wüthrich et al., 2012). DppIV can act on M6P/IGF-IIR to induce ROS production from epithelial cells (Ishibashi et al., 2013), and ROS can induce MMP-2 and MMP-9 production (Rajagopalan et al., 1996). We observed a 3- to 4-fold increase in lung MMP-2 transcript and product in mice infected with WT yeast versus DppIVA RNAi yeast. Elevation in lung MMP2 likely contributes to impaired CCL7 function, as we observed with vaccine strain delivery at the respiratory mucosa (Wüthrich et al., 2012).

Fungal DppIV might also impair the migration of leukocytes during WT infection due to an impaired chemokine gradient. Mammalian DppIV binds fibronectin and collagen and promotes MMP-mediated digestion of extracellular matrix (ECM) (Boonacker and Van Noorden, 2003). Chemokines presented on ECM establish a gradient that facilitates leukocyte migration. DppIV-enhanced destruction of ECM may therefore alter this gradient and impair the normal physiology of leukocyte migration.

One of the most profound effects of fungal DppIVA is its action on mammalian GM-CSF. This cytokine has many functions during the generation of an immune response to pathogens, involving the differentiation and activation of monocytes, macrophages, DCs, and neutrophils (Hamilton, 2008). GM-CSF cleavage by mammalian DppIV inactivates the cytokine, and the cleaved form acts as a high-affinity, competitive inhibitor of intact GM-CSF on its receptor (Broxmeyer et al., 2012). We found that fungal DppIVA likewise cleaves GM-CSF. During in vitro experiments, the expression of DppIVA by yeast protected the pathogen from leukocyte killing by undermining GM-CSF activation of both murine and human macrophages and neutrophils. Likewise, we detected a relative paucity of TipDCs during infection with WT yeast and found that these immune cells, when provided GM-CSF during their development, effectively kill the fungus. GM-CSF's role in defense against pathogens is complex, and its inactivation may have additional effects beyond what we describe here, including DC and macrophage differentiation, leukocyte adhesion, and cytokine production (Hamilton, 2008).

We engineered DsRed reporter yeast to monitor host: pathogen encounters in vivo in the lung during infection. Although TipDCs were potent at killing yeast in vitro and in vivo, these immune cells accounted for only a small fraction of dead yeast in the lung compared to macrophages and especially neutrophils. Neutrophils are a signature feature of the granulomatous inflammatory response to *Blastomyces*, accounting for the characteristic pyogranuloma. Although these cells were most often associated with dead yeast, presumably due to their effector function, there was a striking difference in neutrophil killing of the two fungal strains in vivo, with many more viable WT yeast than DppIVA-silenced yeast. We linked this difference to impaired activation and ROS production by neutrophils in vivo. Since treatment of neutrophils with GM-CSF primes and activates them and enhances their ROS production, it is likely that inactivation of GM-CSF by DppIVA contributes to the defect. However, the blunted influx of $CCR2^+$ monocytes that we observed—in the setting of DppIVA production or in $Ccr2^{-/-}$ mice—also impaired the activation of neutrophils and their in vivo killing of the fungal pathogen. During murine pulmonary Aspergillosis, $CCR2^+$ monocytes and monocyte-derived TipDCs promote neutrophil killing of *Aspergillus* conidia through a mechanism of crosstalk that augments fungicidal action of neutrophils (Espinosa et al., 2014). Although neutrophils pour into the lesions of *Blastomyces* pneumonia, the cells appear to be deprived of the activation signals—GM-CSF and possibly other monocyte-derived signals—needed to eliminate the fungus. Thus, yeast DppIVA acts in at least two ways to foster fungal survival in vivo in the face of neutrophils, by inactivating GM-CSF and impairing recruitment of $CCR2^+$ monocytes and their communication with neutrophils. At least 94 chemokines, cytokines, and immune-modulatory factors are potential targets for DppIV (Ou et al., 2013). Thus, fungal DppIVA cleavage and inactivation of GM-CSF may only be part of its function.

Our study focused on pathogen evasion of innate immunity. However, DppIVA may also undermine adaptive immunity. GM-CSF regulates differentiation of DCs, which bridge innate and adaptive immunity. We previously reported impaired adaptive immunity in response to fungal vaccination in the lung and attributed this defect to exuberant MMP2 and blunted recruitment of inflammatory monocytes (Wüthrich et al., 2012). The combined effect of DppIVA and MMP2 on blunting the number and function of monocyte-derived DCs could together undermine priming of antigen-specific T cells. DppIV could also modulate adaptive immunity by cleaving and inactivating T cell-activating cytokines such as TGF-β, IL-17, and IL-23 or products such as IL-2 (Ou et al., 2013). The many potential DppIV targets and effects their cleavage may have on the immune response to infection indicate multiple ways in which the fungus may dysregulate immunity.

The discovery of fungal DppIVA as a virulence factor makes it a potential therapeutic drug target. The DppIV inhibitor sitagliptin inhibited fungal DppIV activity in vitro, and drug treatment

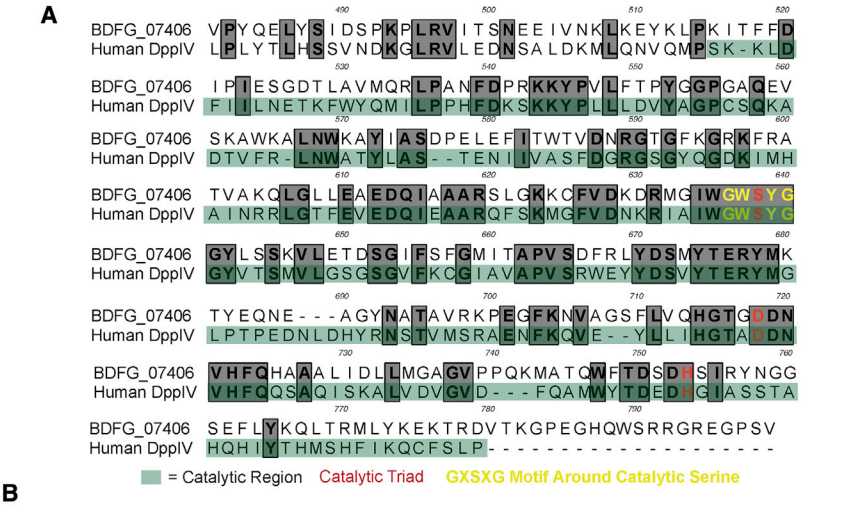

Figure 7. Comparison of *B. dermatitidis* and Human DppIV

(A) Primary amino acid sequence alignment of the catalytic region of *B. dermatitidis* DppIVA (Gene ID: BDFG_07406, Uniprot ID: T5BJB9_AJEDE) and human DppIV (Uniprot ID: P27487), which are 44% identical and 59% similar as determined by NCBI blastp (protein-protein BLAST). Identical amino acids are bolded and boxed in gray.

(B) Top left: 3D model of the previously crystalized human DppIV protein with the catalytic triad (aspartic acid, histidine, serine) boxed. Top center: predicted 3D structure of *B. dermatitidis* DppIVA generated in I-TASSER with the catalytic triad (aspartic acid, histidine, serine) boxed. Top right: overlay of 3D structures of human and *B. dermatitidis* DppIV. Bottom left: zoom in of the human DppIV catalytic triad and (bottom right) *B. dermatitidis* DppIV catalytic triad. All 3D models were made using PyMOL (The PyMOL Molecular Graphics System). See also Figure S7.

ameliorated disease in vivo. Sitagliptin is one of several DppIV inhibitors and was initially approved for human use to treat type 2 diabetes in 2006 (Yazbeck et al., 2009). DppIV inhibitors have been investigated for their ability to treat multiple diseases, including arthritis, multiple sclerosis, and inflammatory bowel disease (Yazbeck et al., 2009). Perhaps inhibitors of DppIV could be repurposed as therapeutic adjuncts for fungal or other infections in which DppIV is found to promote microbial pathogenicity.

DppIV is conserved in mammals and microbes. We compared mammalian and fungal DppIV and found that the amino acid sequences and 3D structures are similar to one another, especially around the active site for catalytic cleavage (Figures 7 and S7). Both of the enzymes likewise cleave at least one substrate similarly, GM-CSF. Many of the separate protease families may have evolved by convergence, but for individual subgroups, including some dipeptidyl peptidases, the genes across phyla seem to have evolved from a common ancestor (Qi et al., 2003). To our knowledge, DppIV has not been described as a fungal virulence factor. DppIV is expressed in *Aspergillus* but has not been studied for a role in pathogenesis. CCL2 and CCR2^{+} cells promote resistance to this pathogen (Espinosa et al., 2014; Morrison et al., 2003), reminiscent of their roles with *Blastomyces*. In *H. capsulatum*, gene deletion of *DppIVA* did not cause a virulence defect (Cooper and Woods, 2009). However, DppIVB is responsible for most of the extracellular DppIV activity and has not been tested for a role in pathogenicity in vivo (Cooper et al., 2009). DppIV has been implicated in the pathogenesis of other infectious diseases such as periodontal disease from *Porphyromonas gingivalis*, Streptococcal toxic shock, and liver disease from Hepatitis C (Casrouge et al., 2011; Ge et al., 2009; Kumagai et al., 2000). Similar peptidases have been studied for their role in Giardia encystation, *Trypanosome* pathogenesis, and malarial release from RBCs (red blood cells) (Antoine-Moussiaux et al., 2009; Arastu-Kapur et al., 2008; Touz et al., 2002). The immune disturbances and progressive disease attributed here to apparent fungal mimicry of mammalian DppIV, in conjunction with the conservation of this ectopeptidase throughout the microbial kingdom, suggest an unappreciated mode of molecular piracy among microbial pathogens.

EXPERIMENTAL PROCEDURES

All work with human cells and animals was approved and conducted according to our institutional IRB and IACUC, respectively.

Mice

C57BL/6 WT mice were obtained from NCI (National Cancer Institute) or Jackson Laboratory. *Ccr2*$^{-/-}$ mice were obtained from Jackson and bred in house. *Csf2ra*$^{-/-}$ mice were provided by Bruce Trapnell, University of Cincinnati.

Fungi

We used *B. dermatitidis* ATCC strain 26199 or 14081 and *H. capsulatum* ATCC strain G217B. See Supplemental Experimental Procedures for growth of strains.

GFP-Sentinel-Silenced Strains

DppIV-silenced (RNAi) and control strains were engineered with the *B. dermatitidis* GFP-sentinel system (Krajaejun et al., 2007). Two nonoverlapping sequences of *DppIV* at the 5′ region and 3′ region (BROAD: BDFG_07406) were targeted for silencing. See Supplemental Experimental Procedures for detail. Vectors for silencing *DppIV* or *GFP* were transformed into *Agrobacterium tumefaciens*. *A. tumefaciens*-mediated transformation (AMT) (Sullivan et al., 2002) was used to transform the 26199-GFP strain with nonsilencing or silencing plasmids to generate a nonsilencing control strain and DppIV-silenced strains, respectively. Silenced transformants were identified by loss of GFP fluorescence and confirmed by DppIV-Glo Protease Assay (Promega).

DsRed Strains

Agrobacterium binary vector construction is described in Supplemental Experimental Procedures. *Agrobacterium* transformation of *B. dermatitidis* strain 26199 with pCAMDsRed#2 and selection for hygromycin resistance were done as described (Sullivan et al., 2002). Transformants were screened for DsRed expression with a BioRad Versadoc 5000 (Green LED, 605 nm filter). Red fluorescent colonies were streaked on selection medium, and isolated colonies were screened by Versadoc and analyzed by fluorescent microscopy and flow cytometry to confirm uniformly fluorescent cells.

Infection

Mice were anesthetized with isoflurane, suspended by their front incisors from a wire, and infected by intubation using a BioLite instrument (Braintree Scientific). Yeasts were given intratracheally (i.t.) by cannula. Some mice were infected i.t. by surgery. Infections were done with 2–3 × 10^4 yeast in 20 μl of PBS per mouse unless noted. Higher inocula were used to assay yeast association with small leukocyte populations or populations with low association with yeast in the lung.

Macrophages

Marrow was collected from femurs and tibias by rinsing and disruption via a 26G needle and filtered via a 40 μM filter. Macrophages were differentiated as in Supplemental Experimental Procedures and cocultured with yeast at a multiplicity of 1:1. At 24 hr postinfection, macrophages were lysed in hypotonic buffer (20 mM Tris HCl, 10 mM NaCl, 3 mM $MgCl_2$ [pH 7.5]), and yeasts plated on HMM agar.

Neutrophils

Neutrophils were purified from bone marrow of 6- to 8-week-old WT mice. Wells contained ratios of neutrophils to yeast of 50 to 100: 1. Some wells received 10 ng/mL GM-CSF. Cocultures were incubated for 6 hr at 37°C and 5% CO_2. Each condition had 6–8 replicates. After cell lysis, yeasts were plated on HMM. Percent killing was defined as (1 − [# of yeast in a condition/# of yeast without neutrophils]) × 100. Neutrophils were depleted with 250 μg α-Ly6g (clone 1A8) (BioXCell) given i.v. (intravenously) every other day.

Ly6C^{hi} Cells

Ly6C^{hi} cells were purified from bone marrow using a two-step approach on the AutoMACS system (Miltenyi) described in Supplemental Experimental Procedures. Ly6C-derived cells were confirmed by flow cytometry. TipDCs generated from Ly6C^{hi}-derived inflammatory DCs produced nitric oxide and TNF-α in response to exposure to yeast (Figure S2B; data not shown), as measured by Griess reaction and/or respective transcript, consistent with TipDCs (Serbina et al., 2003). To test yeast killing in vitro by Ly6C-derived cells, cells were cultured with yeast for 24 hr at 37°C (without GM-CSF) at a ratio of 3:1. For adoptive transfer into *Ccr2*$^{-/-}$ mice, Ly6C^{+}-derived cells were transferred as noted in Supplemental Experimental Procedures.

Csfra2$^{-/-}$ Cells and Experiments

Peritoneal macrophages were obtained by lavage of mice with Hank's balanced salt solution (HBSS) (Corning). Details are in the Supplemental Experimental Procedures. With DppIVA RNAi yeast, 1.5 × 10^6 peritoneal macrophages from WT or *Csf2ra*$^{-/-}$ mice were transferred i.t. into 8- to 12-week-old *Csf2ra*$^{-/-}$ mice just prior to i.t. infection with 3 × 10^4 yeast. With WT yeast, 0.5 × 10^6 peritoneal macrophages from WT or *Csf2ra*$^{-/-}$ mice were transferred i.t. into 8- to 12-week-old *Csf2ra*$^{-/-}$ mice just prior to i.t. infection with 3 × 10^4 yeast.

GM-CSF Neutralization

Mice were given 250 μg of antibody i.v. every other day. We used mAb XMG1.2 (rat IgG1 α-IFN-γ) provided by R. Seder (NIH) and MP1-22E9 (rat IgG2a anti-GM-CSF) with permission of J. Abrams (DNAX). Ascites was made in BALB/c Nu/Nu males. IgG was $(NH_4)_2SO_4$-precipitated and quantified by OD_{280}. Controls received rat IgG (Sigma).

Recombinant DppIVA

Expression of *B. dermatitidis* rDppIVA was performed using EasySelect *Pichia* Expression Kit (Invitrogen). See Supplemental Experimental Procedures for detail.

DppIV GLO Assay

DppIV Glo Protease assays were performed in a 96-well, white-walled, clear-bottom plate as per the manufacturer's protocol (Promega). Details are in Supplemental Experimental Procedures.

Statistical Analysis

p values were calculated by one-way ANOVA with Holm Sidak correction for pairwise multiple comparison. $p < 0.05$ was considered statistically significant. Analysis was performed using Prism software (Graph Pad). Data are presented as means; error bars are SEM.

SUPPLEMENTAL INFORMATION

Supplemental Information includes Supplemental Experimental Procedures and seven figures and can be found with this article online at http://dx.doi.org/10.1016/j.chom.2016.02.001.

AUTHOR CONTRIBUTIONS

A.K.S. and J.L.L. contributed equally to the work. A.K.S., J.L.L., and B.S.K. conceived the experiments. A.K.S. and J.L.L. executed most experiments. T.B. analyzed MS data and produced rDppIVA. M.W. helped in study design and infections. G.S.D. and K.S.V. helped design and perform GM-CSFR and macrophage experiments. J.L.L. and T.D.S. generated DppIVA RNAi strains, and T.B., rDppIVA. T.D.S. generated DsRed strains, and A.K.S. and J.S.F. characterized them. N.H.-S. analyzed cell sources of cytokine. A.K.S. drafted the paper with B.S.K.

ACKNOWLEDGMENTS

This work was supported by NIH R01 AI035681 (B.S.K.), AI093553 (M.W.), and AI106269 (G.S.D.); T32 AI055397 (J.S.F.) and GM007215 (J.L.L.); F32 AI120642 (N.H.-S.); P30ES006096 (K.S.V.); and American Heart 15POST25700182 (K.S.V.). Grzegorz Sabat at UW Biotechnology Center assisted with MS. Karen Ersland shared initial findings on blunted monocyte recruitment by yeast and resistance mediated by CCR2.

Received: June 17, 2015
Revised: December 29, 2015
Accepted: February 1, 2016
Published: February 25, 2016

REFERENCES

Ali, S., Robertson, H., Wain, J.H., Isaacs, J.D., Malik, G., and Kirby, J.A. (2005). A non-glycosaminoglycan-binding variant of CC chemokine ligand 7 (monocyte chemoattractant protein-3) antagonizes chemokine-mediated inflammation. J. Immunol. *175*, 1257–1266.

Antoine-Moussiaux, N., Büscher, P., and Desmecht, D. (2009). Host-parasite interactions in trypanosomiasis: on the way to an antidisease strategy. Infect. Immun. *77*, 1276–1284.

Arastu-Kapur, S., Ponder, E.L., Fonović, U.P., Yeoh, S., Yuan, F., Fonović, M., Grainger, M., Phillips, C.I., Powers, J.C., and Bogyo, M. (2008). Identification of proteases that regulate erythrocyte rupture by the malaria parasite Plasmodium falciparum. Nat. Chem. Biol. *4*, 203–213.

Boonacker, E., and Van Noorden, C.J. (2003). The multifunctional or moonlighting protein CD26/DPPIV. Eur. J. Cell Biol. *82*, 53–73.

Brandhorst, T.T., Roy, R., Wüthrich, M., Nanjappa, S., Filutowicz, H., Galles, K., Tonelli, M., McCaslin, D.R., Satyshur, K., and Klein, B. (2013). Structure and function of a fungal adhesin that binds heparin and mimics thrombospondin-1 by blocking T cell activation and effector function. PLoS Pathog. *9*, e1003464.

Broxmeyer, H.E., Hoggatt, J., O'Leary, H.A., Mantel, C., Chitteti, B.R., Cooper, S., Messina-Graham, S., Hangoc, G., Farag, S., Rohrabaugh, S.L., et al. (2012). Dipeptidylpeptidase 4 negatively regulates colony-stimulating factor activity and stress hematopoiesis. Nat. Med. *18*, 1786–1796.

Carey, B., and Trapnell, B.C. (2010). The molecular basis of pulmonary alveolar proteinosis. Clin. Immunol. *135*, 223–235.

Casrouge, A., Decalf, J., Ahloulay, M., Lababidi, C., Mansour, H., Vallet-Pichard, A., Mallet, V., Mottez, E., Mapes, J., Fontanet, A., et al. (2011). Evidence for an antagonist form of the chemokine CXCL10 in patients chronically infected with HCV. J. Clin. Invest. *121*, 308–317.

Cooper, K.G., and Woods, J.P. (2009). Secreted dipeptidyl peptidase IV activity in the dimorphic fungal pathogen Histoplasma capsulatum. Infect. Immun. *77*, 2447–2454.

Cooper, K.G., Zarnowski, R., and Woods, J.P. (2009). Histoplasma capsulatum encodes a dipeptidyl peptidase active against the mammalian immunoregulatory peptide, substance P. PLoS ONE *4*, e5281.

Espinosa, V., Jhingran, A., Dutta, O., Kasahara, S., Donnelly, R., Du, P., Rosenfeld, J., Leiner, I., Chen, C.C., Ron, Y., et al. (2014). Inflammatory monocytes orchestrate innate antifungal immunity in the lung. PLoS Pathog. *10*, e1003940.

Ge, J., Feng, Y., Ji, H., Zhang, H., Zheng, F., Wang, C., Yin, Z., Pan, X., and Tang, J. (2009). Inactivation of dipeptidyl peptidase IV attenuates the virulence of Streptococcus suis serotype 2 that causes streptococcal toxic shock syndrome. Curr. Microbiol. *59*, 248–255.

Hamilton, J.A. (2008). Colony-stimulating factors in inflammation and autoimmunity. Nat. Rev. Immunol. *8*, 533–544.

Ingmer, H., and Brøndsted, L. (2009). Proteases in bacterial pathogenesis. Res. Microbiol. *160*, 704–710.

Ishibashi, Y., Matsui, T., Maeda, S., Higashimoto, Y., and Yamagishi, S. (2013). Advanced glycation end products evoke endothelial cell damage by stimulating soluble dipeptidyl peptidase-4 production and its interaction with mannose 6-phosphate/insulin-like growth factor II receptor. Cardiovasc. Diabetol. *12*, 125.

Jhingran, A., Mar, K.B., Kumasaka, D.K., Knoblaugh, S.E., Ngo, L.Y., Segal, B.H., Iwakura, Y., Lowell, C.A., Hamerman, J.A., Lin, X., and Hohl, T.M. (2012). Tracing conidial fate and measuring host cell antifungal activity using a reporter of microbial viability in the lung. Cell Rep. *2*, 1762–1773.

Klein, B.S., Vergeront, J.M., Weeks, R.J., Kumar, U.N., Mathai, G., Varkey, B., Kaufman, L., Bradsher, R.W., Stoebig, J.F., and Davis, J.P. (1986). Isolation of Blastomyces dermatitidis in soil associated with a large outbreak of blastomycosis in Wisconsin. N. Engl. J. Med. *314*, 529–534.

Krajaejun, T., Gauthier, G.M., Rappleye, C.A., Sullivan, T.D., and Klein, B.S. (2007). Development and application of a green fluorescent protein sentinel system for identification of RNA interference in Blastomyces dermatitidis illuminates the role of septin in morphogenesis and sporulation. Eukaryot. Cell *6*, 1299–1309.

Kumagai, Y., Konishi, K., Gomi, T., Yagishita, H., Yajima, A., and Yoshikawa, M. (2000). Enzymatic properties of dipeptidyl aminopeptidase IV produced by the periodontal pathogen Porphyromonas gingivalis and its participation in virulence. Infect. Immun. *68*, 716–724.

Morrison, B.E., Park, S.J., Mooney, J.M., and Mehrad, B. (2003). Chemokine-mediated recruitment of NK cells is a critical host defense mechanism in invasive aspergillosis. J. Clin. Invest. *112*, 1862–1870.

Ou, X., O'Leary, H.A., and Broxmeyer, H.E. (2013). Implications of DPP4 modification of proteins that regulate stem/progenitor and more mature cell types. Blood *122*, 161–169.

Pfaller, M.A., and Diekema, D.J. (2010). Epidemiology of invasive mycoses in North America. Crit. Rev. Microbiol. *36*, 1–53.

Qi, S.Y., Riviere, P.J., Trojnar, J., Junien, J.L., and Akinsanya, K.O. (2003). Cloning and characterization of dipeptidyl peptidase 10, a new member of an emerging subgroup of serine proteases. Biochem. J. *373*, 179–189.

Rajagopalan, S., Meng, X.P., Ramasamy, S., Harrison, D.G., and Galis, Z.S. (1996). Reactive oxygen species produced by macrophage-derived foam cells regulate the activity of vascular matrix metalloproteinases in vitro. Implications for atherosclerotic plaque stability. J. Clin. Invest. *98*, 2572–2579.

Rappleye, C.A., and Goldman, W.E. (2008). Fungal stealth technology. Trends Immunol. *29*, 18–24.

Rappleye, C.A., Eissenberg, L.G., and Goldman, W.E. (2007). Histoplasma capsulatum alpha-(1,3)-glucan blocks innate immune recognition by the beta-glucan receptor. Proc. Natl. Acad. Sci. USA *104*, 1366–1370.

Serbina, N.V., Salazar-Mather, T.P., Biron, C.A., Kuziel, W.A., and Pamer, E.G. (2003). TNF/iNOS-producing dendritic cells mediate innate immune defense against bacterial infection. Immunity *19*, 59–70.

Serbina, N.V., Jia, T., Hohl, T.M., and Pamer, E.G. (2008). Monocyte-mediated defense against microbial pathogens. Annu. Rev. Immunol. *26*, 421–452.

Sullivan, T.D., Rooney, P.J., and Klein, B.S. (2002). Agrobacterium tumefaciens integrates transfer DNA into single chromosomal sites of dimorphic fungi and yields homokaryotic progeny from multinucleate yeast. Eukaryot. Cell *1*, 895–905.

Touz, M.C., Nores, M.J., Slavin, I., Piacenza, L., Acosta, D., Carmona, C., and Luján, H.D. (2002). Membrane-associated dipeptidyl peptidase IV is involved in encystation-specific gene expression during Giardia differentiation. Biochem. J. *364*, 703–710.

Ward, J.I., Weeks, M., Allen, D., Hutcheson, R.H., Jr., Anderson, R., Fraser, D.W., Kaufman, L., Ajello, L., and Spickard, A. (1979). Acute histoplasmosis: clinical, epidemiologic and serologic findings of an outbreak associated with exposure to a fallen tree. Am. J. Med. *66*, 587–595.

Wüthrich, M., Ersland, K., Sullivan, T., Galles, K., and Klein, B.S. (2012). Fungi subvert vaccine T cell priming at the respiratory mucosa by preventing chemokine-induced influx of inflammatory monocytes. Immunity *36*, 680–692.

Yazbeck, R., Howarth, G.S., and Abbott, C.A. (2009). Dipeptidyl peptidase inhibitors, an emerging drug class for inflammatory disease? Trends Pharmacol. Sci. *30*, 600–607.

Youseff, B.H., Holbrook, E.D., Smolnycki, K.A., and Rappleye, C.A. (2012). Extracellular superoxide dismutase protects Histoplasma yeast cells from host-derived oxidative stress. PLoS Pathog. *8*, e1002713.